

A Large Indium Sulfide Supertetrahedral Cluster Built from Integration of ZnS-like Tetrahedral Shell with NaCl-like Octahedral Core

Tao Wu,[†] Fan Zuo,[†] Le Wang,[†] Xianhui Bu,[‡] Shou-Tian Zheng,[‡] Richard Ma,[†] and Pingyun Feng^{*,†}

[†]Department of Chemistry, University of California, Riverside, California 92521, United States

[‡]Department of Chemistry and Biochemistry, California State University, 1250 Bellflower Boulevard, Long Beach, California 90840, United States

 Supporting Information

ABSTRACT: An entirely new type of chalcogenide cluster and a new structural mechanism for the formation of large semiconducting tetrahedral clusters have been revealed as a result of crystallization of a templated indium sulfide consisting of an unprecedented cluster, $\text{In}_{38}\text{S}_{65}$, which is the largest supertetrahedral cluster based on trivalent metal ions. At the core of this cluster is $\text{In}_{10}\text{S}_{13}$, which can be considered as a fragment of the NaCl-type lattice. The $\text{In}_{10}\text{S}_{13}$ cluster is coupled to four In_4S_{10} supertetrahedral T2 clusters and four In_3S_3 hexagonal rings to give $\text{In}_{38}\text{S}_{65}$, which is also the largest inorganic chalcogenide supertetrahedral cluster, superseding a supertetrahedral T5 cluster with only 35 metal sites.

Metal chalcogenides have attracted increasing attention because of their diverse technological applications.^{1–3} As an important and newly developed branch of metal chalcogenide materials, crystalline open-framework chalcogenide superlattices with various topologies and compositions occupy a unique interdisciplinary position because such materials are capable of integrating porosity with semiconductivity and are promising for applications ranging from photoelectrochemistry to visible-light-driven photocatalysis.⁴ A special feature of these crystalline porous frameworks is that they are usually constructed from chalcogenide clusters that have precisely defined size and composition.⁵ These chalcogenide clusters represent the smallest possible semiconducting nanoparticles and bridge the size gap between colloidal quantum dot structures and molecular species in solution.⁶

Rational choice of both structure-directing agents and framework compositions on the basis of charge-matching considerations plays a crucial role in determining the types of clusters and their three-dimensional assembly.⁷ Recent studies have led to the development of four series of nanosized supertetrahedral chalcogenide clusters: basic supertetrahedral clusters (T_n), pentasupertetrahedral clusters (P_n), capped supertetrahedral (C_n) clusters, and super-supertetrahedral clusters ($T_{p,q}$), where n , p , and q are integers indicating the size of the clusters (in known clusters, n ranges from 1 to 5 for T_n , 1 to 2 for P_n , and 1 to 3 for C_n).^{5,8–10} All four of these series of supertetrahedral clusters bear a close resemblance to two well-known inorganic structure types of semiconductors, cubic zinc blende and hexagonal wurtzite, both of which adopt tetrahedral coordination for both the cations and the anions.

Among these different series of clusters, basic supertetrahedral T_n clusters are the most fundamental series because they are the exact regular tetrahedron-shaped fragments of the zinc blende-type lattice. The three other series of clusters can be geometrically derived from T_n clusters. Until now, the synthetic strategy for making larger tetrahedral clusters has centered on the use of divalent metal ions (usually Zn^{2+} or Cd^{2+}) to form the cores of the clusters, with the surfaces of the clusters terminated with either organic ligands (e.g., $-\text{SPh}$)¹¹ or higher-valent metal ions such as In^{3+} and Ge^{4+} .

This work demonstrates the existence of new series of supertetrahedral clusters that integrate structural features of the ZnS-type lattice with those of the NaCl-type lattice. It is worth noting that while ZnS-type tetrahedral structures and NaCl-type octahedral structures (e.g., PbS) are well-known, the integration of their tetrahedral and octahedral bonding features in the same chalcogenide tetrahedral clusters has not been observed to date.

Herein we report the novel chalcogenide material ($[\text{In}_{40}\text{S}_{66}(\text{H}_2\text{O})_8]^{12-} \cdot 2\text{Li}^+ \cdot 10(\text{H}^+\text{-DBU}) \cdot 2(\text{CH}_3\text{CN}) \cdot 8(\text{H}_2\text{O})$), denoted as OCF-41 (OCF = organically directed chalcogenide framework), which contains an unprecedented supertetrahedral cluster denoted as a TO2 cluster (where “T” denotes tetrahedral, “O” denotes octahedral, and 2 is the sequence number of this cluster in the series). This cluster features some unusual and unprecedented characteristics, including (1) a NaCl-type octahedral fragment serving as the core of the large tetrahedral cluster and (2) the first example of a Sn_6 octahedron.

OCF-41 was prepared by the solvothermal reaction of $\text{In}(\text{NO}_3)_3$, Li_2S , sodium thiophenolate (NaSPh), 2-amino-1-butanol, acetonitrile, 1,8-diazabicyclo[5.4.0]-7-undecene (DBU), and distilled water at 150 °C for 11 days. Its structure was determined by single-crystal X-ray diffraction (XRD), and the phase purity was supported by powder XRD (Figure S1 in the Supporting Information). NaSPh is essential for the synthesis, even though it is not found in the structure. In addition to affecting the pH of the reactant mixture, which increased from 11.91 to 12.17 following its addition, NaSPh can affect the cluster formation and crystallization through binding to In^{3+} in the solution.

The most unusual structural feature of OCF-41 is its large supertetrahedral cluster, which reveals a new mechanism for the formation of tetrahedral clusters: integration of a NaCl-like octahedral core with a ZnS-like tetrahedral shell (Figure 1). This TO2 cluster consists of an octahedral core ($\text{In}_{10}\text{S}_{13}$) corresponding

Received: July 19, 2011

Published: September 19, 2011

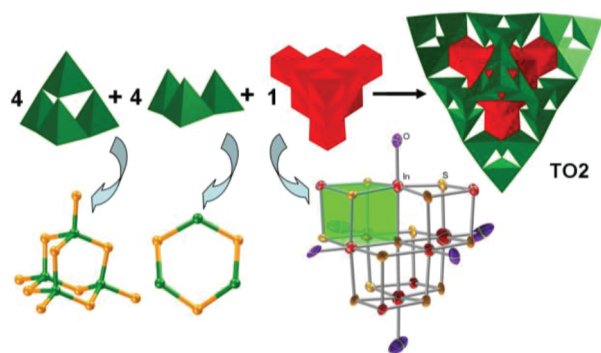


Figure 1. New mechanism for the formation of a large supertetrahedral TO2 cluster constructed from the integration of four classical T2 clusters (In_4S_{10} , green) at the corners, four hexagonal rings (In_3S_3 , green) on the surfaces, and one NaCl-like octahedral core at the center ($\text{In}_{10}\text{S}_{13}$, red).

to one face-centered cubic (fcc) unit cell of the NaCl-type cubic crystal but with four unit-cell corner sites unoccupied. The sulfur sites occupy 12 edge positions and one body-centered position of the fcc cell, and 10 indium sites occupy corners (four occupied and four unoccupied) and six face centers of the fcc cell. It is worth noting that the sixth coordination site for In^{3+} , located at the face center of the $\text{In}_{10}\text{S}_{13}$ cluster, is completed by a H_2O molecule. Alternatively, the $\text{In}_{10}\text{S}_{13}$ cluster can be considered as formed from four tetrahedrally arranged In_4S_4 cubes (similar to the cubane $[\text{4Fe}-\text{4S}]$ cluster¹²) through edge sharing.

At the four corners of the TO2 cluster are four supertetrahedral T2 clusters (In_4S_{10}). The coupling between each T2 cluster and the core $\text{In}_{10}\text{S}_{13}$ cluster involves bonding between the corner In^{3+} site of the $\text{In}_{10}\text{S}_{13}$ cluster and three S^{2-} sites on one face of the T2 cluster, which makes all 10 In^{3+} sites within the $\text{In}_{10}\text{S}_{13}$ clusters octahedrally coordinated. The TO2 cluster is completed through the addition of four $[\text{In}_3\text{S}_3]$ hexagonal rings (one on each face of the TO2 cluster), which provide additional In^{3+} sites to satisfy the bonding requirements of the three corner S^{2-} sites of each of the four T2 clusters and the 12 S^{2-} sites of the $\text{In}_{10}\text{S}_{13}$ cluster. The combination of all these components (one $\text{In}_{10}\text{S}_{13}$ core, four In_4S_{10} T2 clusters, and four In_3S_3 hexagonal rings) gives an overall composition of $[\text{In}_{38}\text{S}_{65}(\text{H}_2\text{O})_6]^{16-}$ for the TO2 cluster.

While such a coupling between supertetrahedral T2 clusters and the $\text{In}_{10}\text{S}_{13}$ cluster is an entirely new mechanism, it is of interest to compare TO2 clusters with other tetrahedral clusters such as T2,2 and P2 clusters that are also based on having four T2 clusters at the corners. In super-supertetrahedral T2,2 clusters (Figure S2a), four T2 clusters are directly interlinked to give a larger cluster with an empty core.¹³ In P2 clusters (e.g., $\text{Li}_4\text{In}_{22}\text{S}_{44}^{18-}$),¹⁴ four corners are similarly occupied by four regular T2 clusters (M_4S_{10}); however, the core of the P2 cluster is a reverse-T2 cluster (S_4M_{10}), which allows face-to-face coupling between the corner T2 cluster and the reverse-T2 cluster through six parallel M–S bonds. (Figure S2b) In addition, the corner In^{3+} sites of the S_4M_{10} reverse-T2 cluster allow the bonding requirements of the corner sulfur sites of the T2 clusters to be met.

Because the TO2 cluster reveals a general pattern for the coupling between the ZnS-type fragment and the NaCl-type fragment, it might be just a member of a potentially large series of clusters yet to be found. While the simplest member can be traced all the way to the biologically important $[\text{4Fe}-\text{4S}]$ cubane cluster, we are particularly interested in clusters involving the

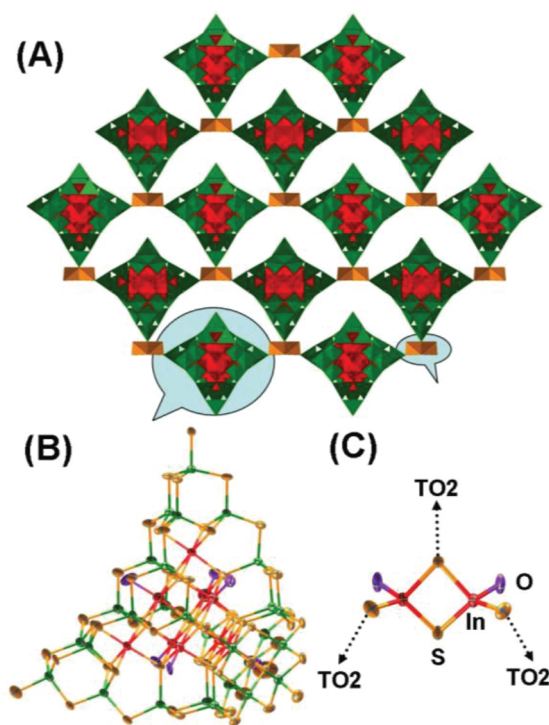


Figure 2. (A) Two-dimensional framework in OCF-41-InS-DBU viewed along a axis. The framework is built from (B) large $\text{In}_{38}\text{S}_{65}(\text{H}_2\text{O})_6$ supertetrahedral TO2 clusters and (C) $\text{In}_2\text{S}(\text{H}_2\text{O})_2$ dimer species. Tetrahedrally coordinated indium cations are shown in green, octahedrally coordinated indium cations in red, S^{2-} in yellow, and oxygen from water in purple.

type of coupling mechanism between the T2 and $\text{In}_{10}\text{S}_{13}$ clusters found in the TO2 cluster. One simpler cluster (denoted here as the TO1 cluster) that bears this type of coupling can be derived by arranging four In_4S_{10} T2 clusters tetrahedrally around one In_4S_4 cube (Figure S3). Four additional In^{3+} sites are also needed (one on each face of the TO1 cluster) to meet the bonding requirements of the corner sulfur sites of the four T2 clusters and the core In_4S_4 cluster, giving an overall formula of $[\text{In}_{24}\text{S}_{44}]^{16-}$ for the TO1 cluster.

The $[\text{In}_{38}\text{S}_{65}(\text{H}_2\text{O})_6]^{16-}$ TO2 clusters in OCF-41 are joined together via dimeric $[\text{In}_2\text{S}(\text{H}_2\text{O})_2]^{4+}$ units to form two-dimensional layers that are further stacked in the ABAB sequence (Figure 2a,b). Each $\text{In}_2\text{S}(\text{H}_2\text{O})_2$ is connected to three TO2 clusters via two indium sites (Figure 2c), and each TO2 cluster in turn is connected with three $\text{In}_2\text{S}(\text{H}_2\text{O})_2$ dimers, giving an overall framework formula of $[\text{In}_{40}\text{S}_{66}(\text{H}_2\text{O})_8]^{12-}$ that is charge-balanced by highly disordered interlayer cations.

The formation of the TO2 cluster results from quite unexpected local coordination geometries for both In^{3+} and S^{2-} . In general, metal cations in supertetrahedral clusters such as T_n , P_n , and C_n are tetrahedrally bonded to chalcogenide anions Q^{2-} ($\text{Q} = \text{S}, \text{Se}$), no matter whether they are mono-, di-, tri-, or tetravalent. In the TO2 cluster, the 28 indium cations at the corners and faces of the cluster still adopt tetrahedral coordination. However, the central part of TO2 the cluster contains 10 octahedrally coordinated indium cations (four InS_6 and six InS_5O units) in which the In–S bond distances range from 2.561 to 2.788 Å, which are significantly longer than the In–S bond distance for tetrahedrally bonded In^{3+} in OCF-41 (2.405–2.494 Å). The average

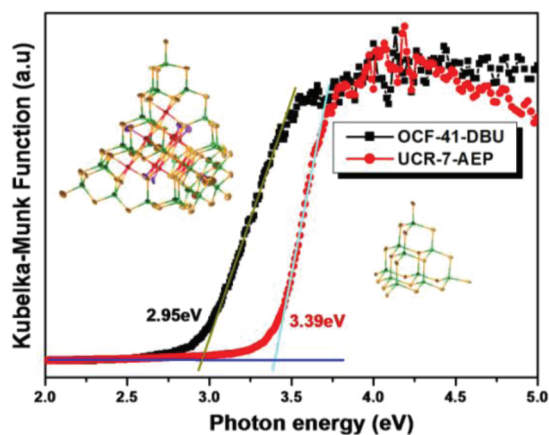


Figure 3. Normalized solid-state UV–vis absorption spectra of OCF-41-InS-DBU with the $\text{In}_{38}\text{S}_{65}$ cluster and UCR-7-InS-AEP with the $\text{In}_{10}\text{S}_{20}$ cluster.

In–O(water) bond distance is 2.251 Å, which is longer than the typical In–O(II) bond length (1.90 Å) but shorter than the average In–S bond distance (2.36 Å).¹⁵

The coordination geometry around the S^{2-} sites in the TO2 cluster is much more exotic. In known supertetrahedral clusters, each S^{2-} site is bonded to two, three, or four metal cations, with the exact coordination number often dependent on the charge of the metal cations. However, sulfide anions in the TO2 cluster adopt four different kinds of bridging modes: μ_2, μ_3, μ_4 , and even μ_6 . The sole $\mu_6\text{-S}^{2-}$ is located at the center of the cluster and is bonded to six In^{3+} sites with bond distances of 2.719–2.788 Å. We are not aware of any literature example in which S^{2-} is bonded to six trivalent metal ions, even through it is not unusual for S^{2-} to bond to six monovalent or divalent ions.¹⁶ In fact, even Sn_4 is generally considered unlikely in the construction of supertetrahedral clusters because of the possibly excessive bond valence sum from trivalent In^{3+} ions to S^{2-} .

To provide a better understanding of the charge distribution on the metal and sulfide sites in the central part of the TO2 cluster, calculation of their bond valence sums (BVSs) and Mulliken charge distributions were carried out. As listed in Table S1, the BVS for the central S^{2-} is 2.078, and the BVSs for the 10 In^{3+} sites ranges from 2.745 to 3.059.

The optical properties of OCF-41 were also studied using solid-state UV–vis–NIR diffuse reflectance spectroscopy, which showed a clear optical transition with a wide band gap of 2.95 eV as determined using Kubelka–Munk methods (Figure 3), indicating that the material retains the semiconducting property of the corresponding pure inorganic dense phase. The transition is likely a result of charge transfer from the S^{2-} -dominated valence band to the In^{3+} -dominated conduction band. In comparison with dense *n*-type semiconductor $\beta\text{-In}_2\text{S}_3$ (band gap 2.1 eV), a relative blue shift of the optical band gap was observed; however, OCF-41 shows a red shift in comparison with UCR-7-AEP (band gap 3.39 eV), which has a twofold-interpenetrated diamond framework with a relatively small T3 cluster ($\text{In}_{10}\text{S}_{20}$) as the building block. Quantum size-confinement effects may be the reason for these observed shifts in optical band gap. The intrinsic semiconducting nature of OCF-41 was also demonstrated by its photocatalytic activity for hydrogen evolution from water in the presence of a Na_2S sacrificial reagent under irradiation with UV–vis light. (Figure S4).

In conclusion, a new supertetrahedral cluster combining structural characteristics of two well-known semiconducting structure types (cubic ZnS and PbS) has been crystallized and structurally characterized. Such a supertetrahedral cluster with a NaCl-type fragment at the core is fundamentally different from recently developed supertetrahedral clusters that are based on cores formed from tetrahedrally coordinated cations and anions. In particular, structural features such as an octahedral core within a tetrahedral cluster and a core made of trivalent metal ions only, which were previously thought to be highly unlikely or not even imagined, have now been realized. The revelation of these new possibilities and a new structural mechanism for the formation of supertetrahedral clusters has fundamentally changed our thinking in regard to the design of such materials, and these materials may also serve as model systems and provide insight into structures of materials (e.g., colloidal quantum dots) that are unsuitable for structural studies via single-crystal XRD.

■ ASSOCIATED CONTENT

S Supporting Information. Experimental preparation, additional figures providing structure descriptions, powder XRD data, and results of BVS and charge distribution calculations. This material is available free of charge via the Internet at <http://pubs.acs.org>.

■ AUTHOR INFORMATION

Corresponding Author

pingyun.feng@ucr.edu.

■ ACKNOWLEDGMENT

We thank the NSF (CHEM-0809335 to P.F. and DMR-0846958 to X.B.) for support of this work. P.Y. is a Camille Dreyfus Teacher Scholar, and X.B. is a Henry Dreyfus Teacher Scholar.

■ REFERENCES

- (1) (a) Kanatzidis, M. G.; Huang, S. P. *Inorg. Chem.* **1989**, *28*, 4667. (b) Mroczek, A.; Kanatzidis, M. G. *Acc. Chem. Res.* **2003**, *36*, 111. (c) Hsu, K. F.; Loo, S.; Guo, F.; Chen, W.; Dyck, J. S.; Uher, C.; Hogan, T.; Polychroniadis, E. K.; Kanatzidis, M. G. *Science* **2004**, *303*, 818. (d) Arachchige, I. U.; Wu, J.; Dravid, V. P.; Kanatzidis, M. G. *Adv. Mater.* **2008**, *20*, 3638. (e) Cook, B. A.; Kramer, M. J.; Harringa, J. L.; Han, M. K.; Chung, D. Y.; Kanatzidis, M. G. *Adv. Funct. Mater.* **2009**, *19*, 1254.
- (2) (a) Kobayakawa, K.; Teranishi, A.; Tsurumaki, T.; Sato, Y.; Fujishima, A. *Electrochim. Acta* **1992**, *37*, 465. (b) Lei, Z.; You, W.; Liu, M.; Zhou, G.; Takata, T.; Hara, M.; Domen, K.; Li, C. *Chem. Commun.* **2003**, 2142. (c) Chen, D.; Ye, J. H. *J. Phys. Chem. Solids* **2007**, *68*, 2317.
- (3) (a) Mohanan, J. L.; Brock, S. L. *J. Non-Cryst. Solids* **2004**, *350*, 1. (b) Mohanan, J. L.; Arachchige, I. U.; Brock, S. L. *Science* **2005**, *307*, 397. (c) Mohanan, J. L.; Brock, S. L. *J. Sol-Gel. Sci. Technol.* **2006**, *40*, 341. (d) Brock, S. L.; Arachchige, I. U.; Kalebaila, K. K. *Comments Inorg. Chem.* **2006**, *27*, 103. (e) Yu, H.; Brock, S. L. *ACS Nano* **2008**, *2*, 1563. (f) Yao, Q.; Arachchige, I. U.; Brock, S. L. *J. Am. Chem. Soc.* **2009**, *131*, 2800. (g) Yao, Q.; Brock, S. L. *Nanotechnology* **2010**, *21*, No. 115502. (h) Pawsey, S.; Kalebaila, K. K.; Moudrakovski, I.; Ripmeester, J. A.; Brock, S. L. *J. Phys. Chem. C* **2010**, *114*, 131871.
- (4) (a) Zheng, N.; Bu, X.; Feng, P. *Nature* **2003**, *426*, 428. (b) Zheng, N.; Bu, X.; Vu, H.; Feng, P. *Angew. Chem., Int. Ed.* **2005**, *44*, 5299. (c) Zhang, Q.; Liu, Y.; Bu, X.; Wu, T.; Feng, P. *Angew. Chem., Int. Ed.* **2008**, *47*, 113. (d) Zhang, Z.; Zhang, J.; Wu, T.; Bu, X.; Feng, P. *J. Am. Chem. Soc.* **2008**, *130*, 15238. (e) Wang, L.; Wu, T.; Zuo, F.; Zhao, X.; Bu, X.; Wu, J.; Feng, P. *J. Am. Chem. Soc.* **2010**, *132*, 3283.

- (5) (a) Bu, X.; Zheng, N.; Feng, P. *Chem.—Eur. J.* **2004**, *10*, 3356. (b) Feng, P.; Bu, X.; Zheng, N. *Acc. Chem. Res.* **2005**, *38*, 293.
- (6) (a) Herron, N.; Calabrese, J. C.; Farneth, W. E.; Wang, Y. *Science* **1993**, *259*, 1426. (b) Zheng, N.; Bu, X.; Lu, H.; Zhang, Q.; Feng, P. *J. Am. Chem. Soc.* **2005**, *127*, 11963. (c) Corrigan, J. F.; Fuhr, O.; Fenske, D. *Adv. Mater.* **2009**, *21*, 1867.
- (7) (a) Wu, T.; Wang, X. Q.; Bu, X.; Zhao, X.; Wang, L.; Feng, P. *Angew. Chem., Int. Ed.* **2009**, *48*, 7204. (b) Wu, T.; Wang, L.; Bu, X.; Chau, V.; Feng, P. *J. Am. Chem. Soc.* **2010**, *132*, 10823. (c) Wu, T.; Khazhaky, R.; Wang, L.; Bu, X.; Zheng, S.; Chau, V.; Feng, P. *Angew. Chem., Int. Ed.* **2011**, *50*, 2536. (d) Wu, T.; Bu, X.; Zhao, X.; Khazhaky, R.; Feng, P. *J. Am. Chem. Soc.* **2011**, *133*, 9616.
- (8) (a) Zimmermann, C.; Melullis, M.; Dehnen, S. *Angew. Chem., Int. Ed.* **2002**, *41*, 4269. (b) Dehnen, S.; Brandmayer, M. K. *J. Am. Chem. Soc.* **2003**, *125*, 6618. (c) Zimmermann, C.; Anson, C. E.; Weigend, F.; Clérac, R.; Dehnen, S. *Inorg. Chem.* **2005**, *44*, 5686. (d) Dehnen, S.; Melullis, M. *Coord. Chem. Rev.* **2007**, *251*, 1259.
- (9) (a) Li, H.; Laine, A.; O'Keeffe, M.; Yaghi, O. M. *Science* **1999**, *283*, 1145. (b) Li, H.; Eddaoudi, M.; Laine, A.; O'Keeffe, M.; Yaghi, O. M. *J. Am. Chem. Soc.* **1999**, *121*, 6096. (c) Li, H.; Kim, J.; Groy, T. L.; O'Keeffe, M.; Yaghi, O. M. *J. Am. Chem. Soc.* **2001**, *123*, 4867. (d) Li, H.; Kim, J.; O'Keeffe, M.; Yaghi, O. M. *Angew. Chem., Int. Ed.* **2003**, *42*, 1819.
- (10) (a) Vaqueiro, P. *Inorg. Chem.* **2008**, *47*, 20. (b) Vaqueiro, P.; Romero, M. L. *J. Phys. Chem. Solids* **2006**, *68*, 1239. (c) Vaqueiro, P.; Romero, M. L. *Chem. Commun.* **2007**, 3282. (d) Vaqueiro, P.; Romero, M. L. *Inorg. Chem.* **2009**, *48*, 810.
- (11) (a) Lee, G. S. H.; Craig, D. C.; Ma, I.; Scudder, M. L.; Bailey, T. D.; Dance, I. G. *J. Am. Chem. Soc.* **1988**, *110*, 4863. (b) Dance, I. G.; Fisher, K. G. *Prog. Inorg. Chem.* **1994**, *41*, 637. (c) Fenske, D.; Zhu, N.; Langetepe, T. *Angew. Chem., Int. Ed.* **1998**, *37*, 2640. (d) Soloviev, V. N.; Eichhofer, A.; Fenske, D.; Banin, U. *J. Am. Chem. Soc.* **2001**, *123*, 2354. (e) Dehnen, S.; Eichhofer, A.; Fenske, D. *Eur. J. Inorg. Chem.* **2002**, 279.
- (12) Stack, T. D. P.; Holm, R. H. *J. Am. Chem. Soc.* **1987**, *109*, 2546.
- (13) Zheng, N.; Bu, X.; Wang, B.; Feng, P. *Science* **2002**, *298*, 2366.
- (14) Zheng, N.; Bu, X.; Feng, P. *Angew. Chem., Int. Ed.* **2004**, *43*, 4753.
- (15) Brese, N. E.; O'Keeffe, M. *Acta Crystallogr.* **1991**, *B47*, 192.
- (16) (a) Wang, X.-J.; Langetepe, T.; Persau, C.; Kang, B.-S.; Sheldrick, G. M.; Fenske, D. *Angew. Chem., Int. Ed.* **2002**, *41*, 3818. (b) Chitsaz, S.; Fenske, D.; Fuhr, O. *Angew. Chem., Int. Ed.* **2006**, *45*, 8055. (c) Berlinguette, C. P.; Holm, R. H. *J. Am. Chem. Soc.* **2006**, *128*, 11993.